MIMS Majalah Ilmiah Matematika dan Statistika 25 (1), 2025, 22 – 35
eISSN 2722-9866 pISSN 1411-6669
https://mims.jurnal.unej.ac.id/index.php/MIMS/index

# Chaotic outbreak in discrete epidemic model with vaccination and quarantine interventions and limited medical resources

**Faizal Rifky Fahreza[1], Moh Hasan[1]*, Kiswara Agung Santoso[1]**

[1]Department of Mathematics, University of Jember

*Correspondence: hasan.fmipa@unej.ac.id

Received: 16-02-2025, accepted: 26-03-2025

## Abstract

The spread of infectious diseases can be analyzed dynamically using a discrete dynamic system. The characteristics of the infectious disease phenomenon are interesting to study as parameters considered in a dynamic system. Some of these include vaccination interventions, quarantine, or even an open condition such as limited medical resources. Analysis of a discrete epidemic model system with those three factors can be conducted to understand each of their impacts on the dynamics of disease spread within a population or even to determine the potential for a chaotic outbreak. In this study, an epidemiological model was formulated considering these three factors. Numerical simulations were also conducted to directly observe the influence of these three factors on the dynamics of disease spread. Additionally, efforts to control chaos were also implemented in the system. The limitation of medical resources affects the spread of diseases. Because the coverage of medical resources is limited, it can cause a high surge in cases within the population. This phenomenon of case surges can subsequently be mitigated by vaccination parameters such as vaccine efficacy and the rate of vaccine distribution within the population. Furthermore, the formulated system has the potential to exhibit chaotic behavior when the infection rate increases, in other words, the disease becomes an uncontrollable and unpredictable epidemic. Next, the thing that can be done to suppress this chaotic phenomenon is to directly intervene in the rate of disease spread within the population.

**Keywords:** Epidemic model, chaos, bifurcation
**MSC2020:** 39A33

## 1. Introduction

Discrete dynamic systems describe phenomena using discrete time, with the logistic map as a key example. In biology, these systems are applied to study mosquito control [1], predator-prey dynamics considering the Allee effect [2], [3], and disease spread [4], [5]. In economics, they help analyze macroeconomic dynamics and control strategies [6]. The analysis is often supported by theories such as bifurcation and chaos theory.

Bifurcation in a dynamic system describes how the behavior of the system changes in response to a change in the parameters within the system. Many studies have examined bifurcation in discrete dynamical systems. Studies that have been extensively conducted

include the analysis of the existence of bifurcations in a discrete system, whether period-doubling bifurcation or Neimark-Sacker bifurcation [4], [7], [8]. Additionally, bifurcation analysis can also be conducted to find the existence of common bifurcations in discrete systems such as transcritical, pitchfork, or saddle node [8], [9]. Furthermore, bifurcations that occur in a discrete system under certain scenarios can lead to chaotic behavior. The chaotic behavior of a discrete system can later be analyzed using chaos theory.

Chaos theory explains systems that behave erratically. Previous studies have been extensively conducted to analyze whether the system has chaotic potential. The analysis of chaotic behavior in discrete systems is often conducted using the maximum Lyapunov exponent. Then, the chaotic behavior that emerges in discrete systems can also be controlled to stabilize the system [10], [11]. The study of chaos control in a discrete system can be applied to cases such as turbulence, weather forecasting, population dynamics, cardiology, chemical reactions, or others. In addition, studies on the analysis of discrete systems using chaos theory or bifurcation theory on discrete systems are also interesting to conduct in cases of disease spread.

Numerous studies have explored the dynamic systems of disease spread, starting with the Kermack-McKendrick model for simple transmission. As our understanding of diseases has advanced, these analyses have been increasingly employed to evaluate intervention measures like vaccination and quarantine [12], [13]. They also help identify when herd immunity occurs in a population [14], [15] and examine the effects of individual mobility on disease transmission [16].

Covid-19 is still a current disease, as shown by updates on the WHO website about new positive cases. This disease began at the end of 2019 and became a global pandemic [17]. It is interesting to study Covid-19 using discrete dynamic systems. Many medical and non-medical strategies have been used to control its spread, with vaccination and quarantine being two common approaches [18], [19]. A challenging reality is the limited number of healthcare workers and facilities, which significantly impacts the pandemic's effects. We can create a dynamic system model by looking at these interventions and the limits of medical resources. Analyzing this Covid-19 dynamic system can help us understand its potential for chaos, what happens during chaos, and how existing interventions influence its spread.

This study will analyze the dynamic system of Covid-19 spread, focusing on vaccination and quarantine interventions and the constraints of limited medical resources. We will utilize the model developed by Fahreza et al., 2023 [20], which will be reformulated to account for these resource limitations. A numerical simulation will then be conducted to assess the potential for chaotic behavior in the system, and we will explore the consequences of such chaos, as well as methods for controlling it when it occurs.

## 2. Methods

The model used in this study will reformulate the existing model in [20], where the Covid-19 epidemic model with vaccination and quarantine interventions is stated as follows:

$$\begin{aligned}
\frac{dS}{dt} &= \Lambda - \frac{\lambda SI}{N} - \frac{\lambda qSQ}{N} - \varphi_1 S + \rho R - \mu S,\\
\frac{dV_1}{dt} &= \varphi_1 S - \frac{\lambda pV_1 I}{N} - \frac{\lambda pqV_1 Q}{N} - \varphi_2 V_1 - \mu V_1,\\
\frac{dV_2}{dt} &= \varphi_2 V_1 - \frac{\lambda rV_2 I}{N} - \frac{\lambda rqV_2 Q}{N} - \mu V_2,\\
\frac{dI}{dt} &= \frac{\lambda SI}{N} + \frac{\lambda pV_1 I}{N} + \frac{\lambda rV_2 I}{N} + \frac{\lambda qSQ}{N} + \frac{\lambda pqV_1 Q}{N} + \frac{\lambda rqV_2 Q}{N} - \tau_1 I + \tau_2 Q - \gamma I - \zeta I - \mu I,\\
\frac{dQ}{dt} &= \tau_1 I - \tau_2 Q - \gamma Q - \zeta dQ - \mu Q,\\
\frac{dR}{dt} &= \gamma I + \gamma Q - \rho R - \mu R,\\
\frac{dD}{dt} &= \zeta I + \zeta dQ,\\
N &= S + V_1 + V_2 + I + Q + R + D,
\end{aligned} \tag{1}$$

The compartment $S(t)$ represents the susceptible population, while $V_1(t)$ and $V_2(t)$ indicate those who have received one and two doses of vaccination, respectively. $I(t)$ refers to individuals exposed to the disease with moderate to severe symptoms requiring medical intervention, while $Q(t)$ denotes those with mild symptoms manageable through self-quarantine. $R(t)$ signifies the recovered population, and $D(t)$ represents those who have died from the disease. A summary of the parameters is provided in Table 1.

Table 1. Parameter in Model (1)

| Parameters | Descriptions | Parameters | Descriptions |
|---|---|---|---|
| $\lambda$ | Infection rate | $\rho$ | Reinfection rate |
| $\varphi_1$ | First dose vaccination rate | $p$ | Reduction in the infection rate due to the first dose of vaccination |
| $\varphi_2$ | Second dose vaccination rate | $r$ | Reduction in the infection rate due to the second dose vaccination |
| $\tau_1$ | The rate of transfer $I(t)$ to $Q(t)$ | $q$ | Reduction in the infection rate due to quarantine |
| $\gamma$ | Recovery rate | $d$ | Reduction in disease mortality rates due to vaccines |
| $\zeta$ | Disease mortality rate | $\Lambda$ | Normal birth rate |
| $\tau_2$ | The rate of transfer $Q(t)$ to $I(t)$ | $\mu$ | Normal mortality rate |

Model (1) will be formulated by transforming it into a discrete form and incorporating conditions that can illustrate the limitations of medical resources. Next, numerical simulations will be conducted to explore the dynamics occurring in the system, such as the emergence of bifurcations and chaotic behavior within the system.

# 3. Results

## 3.1 Model Formulation

Model (1), which is a continuous dynamic system, will first be transformed into a discrete dynamic system. Look back at Model (1), first we will take one compartment, namely the compartment $S(t)$. Let the number of compartments $S(t)$ be denoted as $S_t$. Based on the compartment $S(t)$, we know that the right-hand side of this compartment indicates changes in this compartment, where the changes in the compartment are more clearly given every t expressed in days. As a result, the changes occurring in one day $(t)$ in the compartment $S(t)$ can be expressed as follows:

$$S_{t+1} - S_t = \Lambda - \frac{\lambda S_t I_t}{N_t} - \frac{\lambda q S_t Q_t}{N_t} - \varphi_1 S_t + \rho R_t - \mu S_t.$$

Thus, for the discrete form of the compartment $S(t)$, we can write it as follows:

$$S_{t+1} = S_t + \left(\Lambda - \frac{\lambda S_t I_t}{N_t} - \frac{\lambda q S_t Q_t}{N_t} - \varphi_1 S_t + \rho R_t - \mu S_t\right). \quad (2)$$

This also applies to all compartments in Model (1).

Model (1) uses the standard incidence rate, suitable for field conditions where population density is unaffected by population size. However, this study will employ a framework that better represents population density, which is significantly influenced by population size. Thus, the incidence rate for this model will be as follows: [21]

$$\lambda S(t) I(t) \quad (3)$$

Then, by applying the incidence rate of Equation (3) to Model (1), the equation form in the compartment $S(t)$ is obtained as follows:

$$\frac{dS}{dt} = \Lambda - \lambda SI - \lambda q SQ - \varphi_1 S + \rho R - \mu S. \quad (4)$$

This will also be applied to other compartments.

Next, we will formulate Model (1) to illustrate the limitations of medical resources. This model focuses on the population needing additional medical intervention, specifically those with moderate to severe symptoms (compartment $I(t)$). Key considerations include the limited availability of healthcare facilities and personnel, as well as how medical interventions can aid recovery. If the number of individuals with moderate to severe symptoms exceeds the available medical resources in an area, some may not receive necessary care.

Two conditions will be established for changes in compartment $I(t)$: when the population is below and when it exceeds the medical resource threshold, $I_b$. For the condition where the infected population is below this threshold, the entire group will receive medical

intervention. The normal recovery rate without intervention is $\gamma_n$, while the recovery rate with intervention is $\gamma_m$. The changes under these conditions can be summarized as follows:

$$f(I_t) = (\gamma_n + \gamma_m)I_t. \tag{5}$$

In the second condition, when the population exceeds local medical resources, only a number equal to the threshold can receive treatment. The remaining individuals will recover at a standard rate or without intervention. Thus, this scenario can be summarized as follows:

$$f(I_t) = (\gamma_n + \gamma_m)I_b + \gamma_n(I_t - I_b). \tag{6}$$

After formulating the model by adding the previously provided assumptions. What is obtained from Equations (2), (4), (5), and (6) will be applied to Model (1). Thus, a discrete epidemic model with vaccination and quarantine interventions, as well as limitations on medical resources, will be used in this study as shown in the following Equation (7):

$$\begin{aligned}
S_{t+1} &= S_t + \Lambda - \lambda S_t I_t - \lambda q S_t Q_t - \varphi_1 S_t + \rho R_t - \mu S_t,\\
V_{1_{t+1}} &= V_{1_t} + \varphi_1 S_t - \lambda p V_{1_t} I_t - \lambda pq V_{1_t} Q_t - \varphi_2 V_{1_t} - \mu V_{1_t},\\
V_{2_{t+1}} &= V_{2_t} + \varphi_2 V_{1_t} - \lambda r V_{2_t} I_t - \lambda rq V_{2_t} Q_t - \mu V_{2_t},\\
I_{t+1} &= I_t + \lambda S_t I_t + \lambda p V_{1_t} I_t + \lambda r V_{2_t} I_t + \lambda q S_t Q_t + \lambda pq V_{1_t} Q_t + \lambda rq V_{2_t} Q_t - \tau_1 I_t + \tau_2 Q_t - \mu I_t - \zeta I_t\\
&\quad - f(I_t),\\
Q_{t+1} &= Q_t + \tau_1 I_t - \tau_2 Q_t - \gamma_n Q_t - \zeta d Q_t - \mu Q_t,\\
R_{t+1} &= R_t + \gamma_n Q_t - \rho R_t - \mu R_t + f(I_t),\\
D_{t+1} &= D_t + \zeta I_t + \zeta d Q_t,
\end{aligned} \tag{7}$$

with,

$$f(I_t) = \begin{cases} (\gamma_n + \gamma_m)I_t, & I_t \le I_b \\ (\gamma_n + \gamma_m)I_b + \gamma_n(I_t - I_b), & I_t > I_b. \end{cases}$$

### 3.2 Numerical Simulation

Numerical simulations are conducted to investigate the system's behavior with an initial value and how dynamics change as parameters are varied. First, a simulation will explore the periodic solution, which will provide insights into the compartment values over time. The parameter values will be defined, and those used for the periodic solution of System (7) are presented in Table 2 below:

Table 2. The values of the parameters

| Parameters | Value | Parameters | Value | Parameters | Value |
|---|---|---|---|---|---|
| $\lambda$ | 0.5 | $\rho$ | 0.0065 | $\zeta$ | 0.001 |
| $\varphi_1$ | 0.2 | $p$ | 0.590071 | $\tau_2$ | 0.05 |
| $\varphi_2$ | 0.1 | $r$ | 0.180143 | $\gamma_m$ | 0.25 |
| $\tau_1$ | 0.15 | $q$ | 0.05 | $\Lambda$ | $\mu N$ |
| $\gamma_n$ | 0.0015 | $d$ | 0.02 | $\mu$ | 0.3 |
| $I_b$ | 0.2 | | | | |

Then the initial values for each compartment are provided in Table 3:

Table 3. Initial value of the System (7) compartment

| Compartment | Initial Value | Compartment | Initial Value |
|---|---|---|---|
| $S$ | 0.7 | $Q$ | 0.025 |
| $V_1$ | 0.12 | $R$ | 0.018 |
| $V_2$ | 0.08 | $D$ | 0.007 |
| $I$ | 0.05 | | |

Based on the initial values in Table 3, the total population $(N)$ in this simulation is obtained as $N = S + V_1 + V_2 + I + Q + R + D = 1$.

Next, the dynamics of the periodic solution of System (7) will be shown in the infected compartment $(I)$.

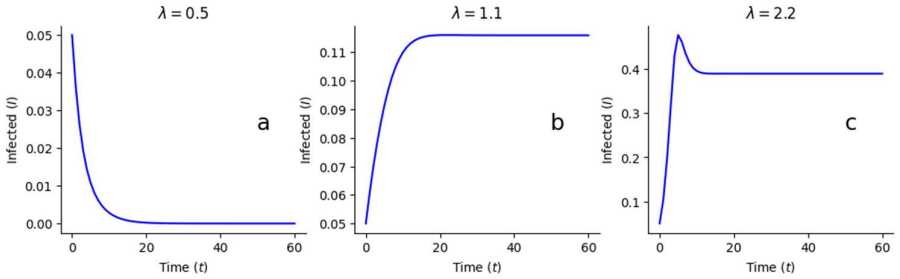


Figure 1. Periodic solution of System (7) a. $\lambda = 0.5$ b.$\lambda = 1.1$ c.$\lambda = 2.2$

Figure 1a shows the periodic solution of the infected compartment in System (7) with parameters from Table 2. Over a 60-day period, the infected population trends toward stability in a disease-free state, indicating that the infectious disease could diminish over time and not escalate into an epidemic. In contrast, Figure 1b depicts the effect of a higher infection rate of $(\lambda = 1.1)$, resulting in an endemic equilibrium state. This means the disease will persist as long as the parameters remain unchanged. Overall, these two periodic solutions highlight how the infection rate can shift the system's behavior from stability to a disease-free condition and ultimately to an endemic state.

Upon examining Figure 1b, it is evident that the increase in infection cases has not yet surpassed the medical resources threshold $(I_b = 0.2)$. A simulation will be conducted by increasing the infection rate to see if the dynamics can exceed this threshold. Figure 1c depicts the periodic solution of compartment $I$ at an infection rate of $\lambda = 2.2$, showcasing a scenario where the infectious disease spreads beyond medical resource capacity. While a surge in cases occurs, it can still be suppressed, allowing compartment $I$ to stabilize. The stable point identified in Simulation $I$ remains above the threshold $(I_b)$, prompting further exploration of how changes in the infection rate $(\lambda)$ affect the system's stability conditions.

The change in the infection rate with respect to stability will be presented using a bifurcation diagram. First, the bifurcation diagram of the system between $\lambda$ and $I$ will be presented if the parameter values are given as in Table 2.

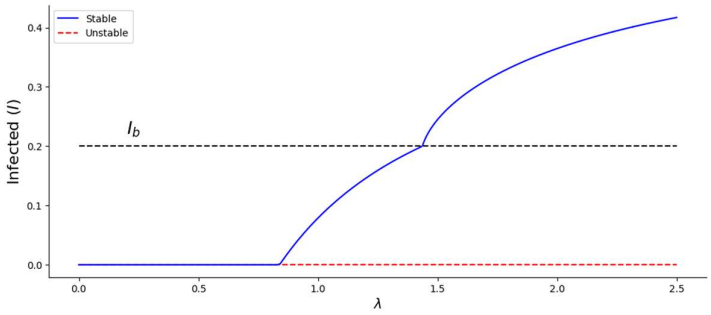


Figure 2. Bifurcation diagram of System (7)

Figure 2 illustrates how the dynamics of compartment $I$ relate to the value of λ. Limited medical resources increase the rate of case growth, as shown by λ's trend pushing equilibrium $I$ toward the threshold. Despite reaching a higher equilibrium point, the stable condition indicates that this phenomenon remains manageable. Next, we will investigate how changing the threshold value $I_b$ affects the system's dynamics.

The threshold value for medical resources, $(I_b)$, will be modified in the next simulation. Currently, $I_b = 0.2$ indicates that resources can handle only 20% of the population. The goal is to increase this threshold until it can support 50% of the total population.

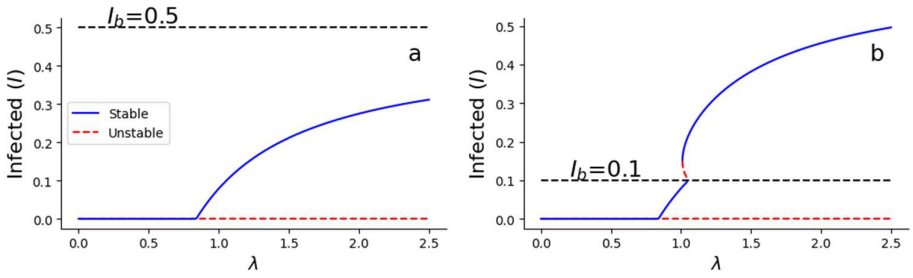


Figure 3. Bifurcation diagram of System (7) a. $I_b = 0.5$ b. $I_b = 0.1$

Figure 3a illustrates the dynamics of I against λ when medical resources can aid the recovery of up to 50% of the population. Compartment $I$ does not reach the threshold, showing a flattening trend, suggesting that the spread of infectious diseases is likely controllable.

We examine the decrease in the threshold of medical resources that can accommodate only 10% of the total population. Figure 3b illustrates the dynamics of $I$ in relation to λ when$I_b = 0.1$. When $I$ exceeds the threshold, a backward bifurcation occurs, complicating control as the number of infected individuals surges. The next section will describe how the system's periodic solution behaves as λ approaches the threshold.

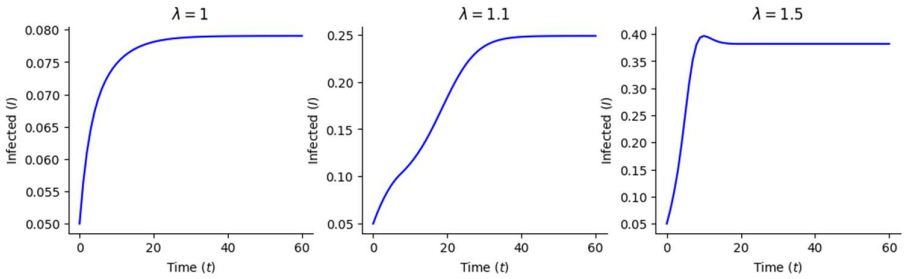


Figure 4. Periodic solution of system (7) when $I_b = 0.1$

Figure 4 illustrates that the system can face a significant surge in infection cases due to limited medical resources. This scarcity, combined with a sudden spike in cases, complicates efforts to achieve a disease-free state. The variations in the $I_b$ values suggest that the availability of medical resources is essential for managing infectious diseases. Additionally, System (7) considers the effects of vaccination and quarantine interventions, prompting the next step to explore how these measures impact the system, particularly given that its medical capacity can only support 10% of the population.

Exploration will be conducted by reviewing the bifurcation diagram of compartment $I$ with respect to several parameters related to vaccination and quarantine interventions. Assume System (7) has $\lambda = 1.1$, resulting in the following bifurcation diagram:

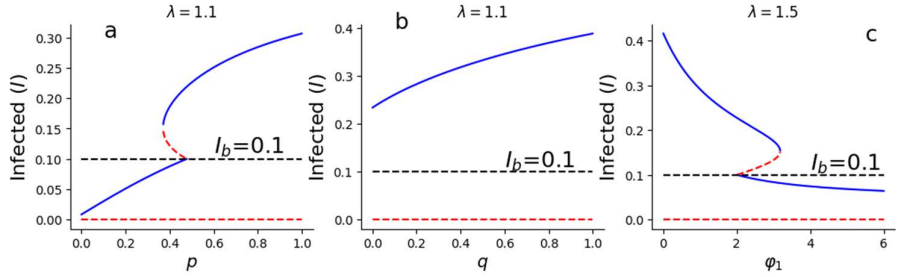


Figure 5. Bifurcation diagram between $I$ and a. $p$ b. $q$ c. $\varphi_1$

Figures 5a and 5b illustrate how the dynamics of $I$ relate to the parameters $p$, representing vaccine efficacy, and $q$, indicating the proportion of individuals adhering to quarantine measures [20]. Increasing these parameters can reduce the equilibrium level of $I$, but efforts related to $q$ have not yet brought the system below the $I_b$ threshold. This suggests that improving vaccine efficacy can help manage a population that medical resources can only support up to 10%. Additionally, quarantine measures have proven inadequate in lowering the system's conditions beneath the threshold. Notably, Figures 5a and 5b assume $\lambda = 1.1$, while those in Figure 3b remain just above the threshold.

If $\lambda$ is significantly above the threshold, such as $\lambda = 1.5$, the intervention parameter to consider is $\varphi_1$, or the vaccination rate. Figure 5c illustrates that increasing this rate can bring the system's equilibrium below the threshold$I_b$. Despite the challenges of disease

spread, vaccination interventions can still be effective, though the size of the infected population must be considered. In certain situations, boosting vaccine efficacy or accelerating vaccine administration may be necessary when it can no longer contain compartment $I$.

After exploring with $I_b$, we will return to explore System (7) by increasing the value of λ or the infection rate. The threshold value of $I_b$ will again use the assumption that medical resources are available for 20% of the population.

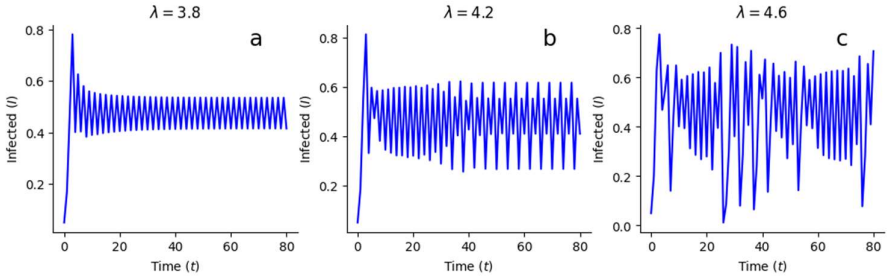


Figure 6. Periodic solution of System (7) a.$\lambda = 3.8$ b.$\lambda = 4.2$ c.$\lambda = 4.6$

The value of λ is first increased to 3.8, as shown in Figure 6a, where the periodic solution indicates that $I$ stabilizes towards two equilibrium points or undergoes period-doubling. When λ rises to 4.2, Figure 6b reveals that System (7) stabilizes towards four equilibrium points, again demonstrating period-doubling. This phenomenon is a pathway to chaos. Figure 6c illustrates the system's attraction to multiple attractors, a behavior characteristic of chaotic conditions. Thus, the potential for chaos in System (7) will be further investigated.

The chaotic behavior in the system can be investigated using the Period-Doubling bifurcation diagram up to the Maximum Lyapunov Exponent. Figure 6 has shown the presence of period-doubling behavior in the system, with the continuous increase of the value of λ, the Period-Doubling bifurcation diagram is obtained as follows:

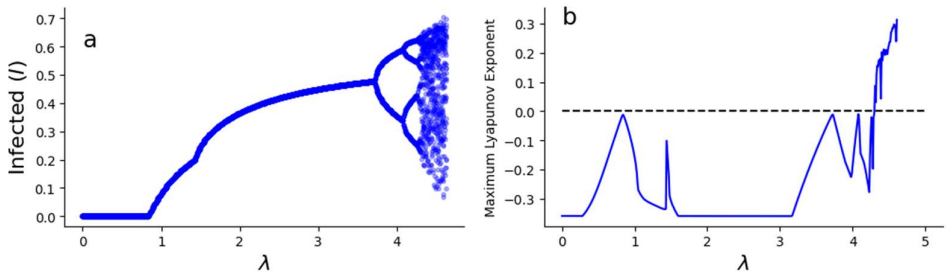


Figure 7. a. Bifurcation diagram of System (7) b.*Maximum Lyapunov Exponent* of System (7)

Figure 7a shows that as λ increases, period-doubling continues, leading to multiple attractors and the potential for chaotic behavior. Maximum Lyapunov Exponent (MLE)

analysis further confirms this chaos. Figure 7b illustrates the MLE values at each λ; positive MLE indicates chaos, while an MLE of 0 points to bifurcation. It is clear from the data that the system has many attractors with positive MLE values, confirming that System (7) exhibits chaotic behavior in this region.

Chaotic behavior in the system can also be demonstrated by its sensitivity to initial values. The periodic solution of System (7) that exhibits chaos will be presented if a perturbation of $10^{-4}$ is applied to its initial value (Table 3).

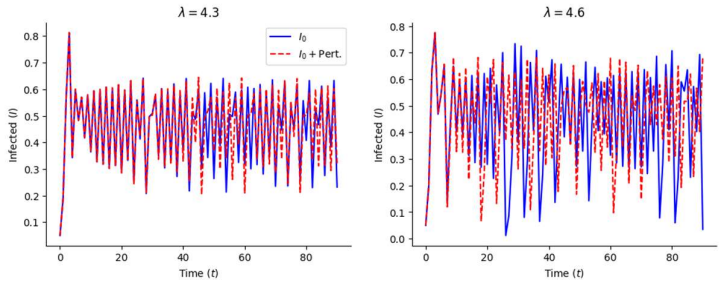


Figure 8. Periodic solution of System (7) during chaos

Figure 8 shows the periodic solution of the system for two λ values that are similarly sensitive to initial conditions. The chaotic behavior in the disease spread model indicates a highly uncontrollable phenomenon. Daily fluctuations in the infected population hinder predictions about when disease transmission will peak or end. Another chaotic scenario will be presented, focusing on cases where medical resources can manage only 10% of the population.

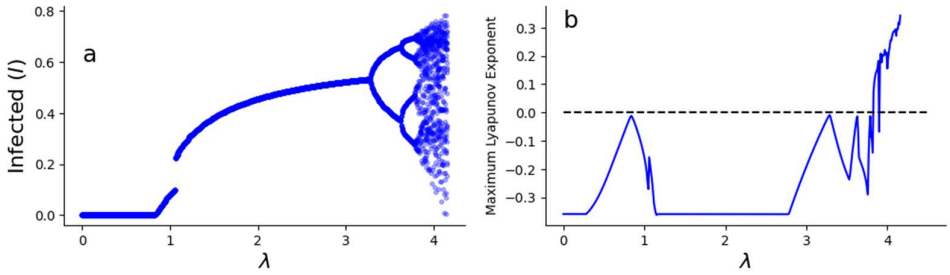


Figure 9. a. Bifurcation diagram dan b. Maximum Lyapunov Exponent System at $I_b = 0.1$

Figure 9 shows that bifurcation at low medical resource thresholds can lead to chaos. Simulations indicate that exceeding these thresholds may result in chaotic behavior. Therefore, proactive measures to control the infection rate are essential to prevent a chaotic outbreak.

Chaotic behavior in the phase diagram leads to a limit cycle, or Neimark-Sacker bifurcation. A simulation shows changes as λ varies, using parameters from Table 2, with vaccine infection rates $\varphi_1 = 1.1$ and $\varphi_2 = 1.3$, and a medical resource threshold of 50%.

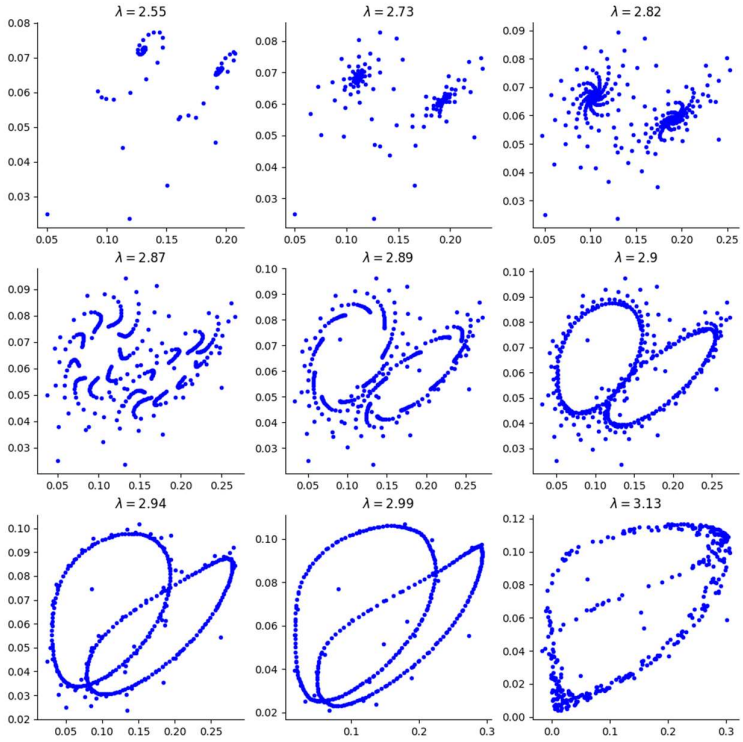


Figure 10. Phase diagram System (7)

Figure 10 shows that as λ increases, the system maintains a close invariant, indicating a Neimark-Sacker bifurcation. During this close invariant behavior, periodic solutions emerge, characterized by a repeating pattern.

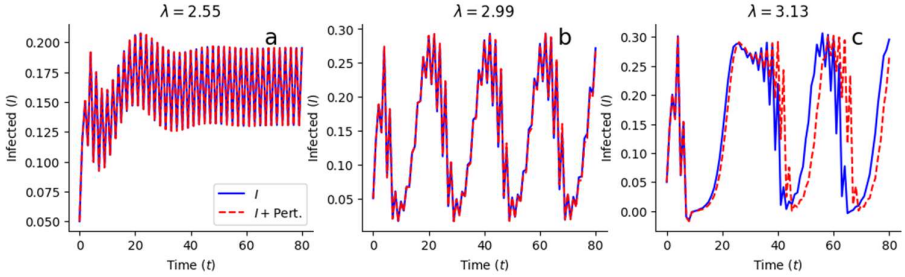


Figure 11. Periodic solution of system (7) a.$\lambda = 2.55$ b.$\lambda = 2.99$ c.$\lambda = 3.13$

Figure 11a depicts the system's solution during period doubling. When a close invariant ($\lambda = 2.99$) is present, the periodic solution establishes a repeating pattern, as seen in Figure 11b. Additionally, the figure illustrates the system's response to perturbations, indicating that the system within a closed invariant is not sensitive to initial value variations.

Figure 11c shows the deviation of the periodic solution when the system is operational, highlighting its sensitivity to initial conditions. Consequently, the system exhibits chaotic

behavior, despite maintaining a recognizable pattern for a time.

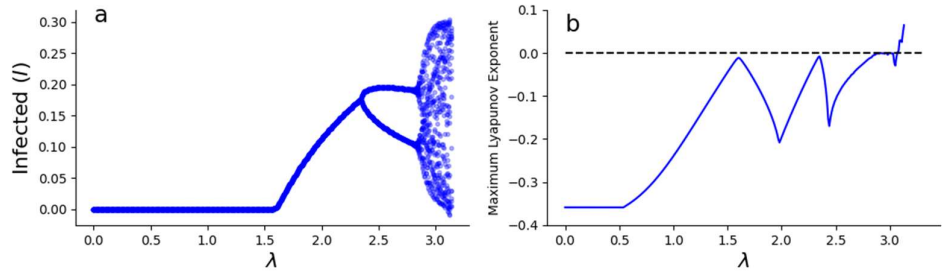


Figure 12. a.Bifurcation diagram b.Maximum Lyapunov Exponent at $\varphi_1 = 1.1$, $\varphi_2 = 1.3$, and $I_b = 0.5$

Figure 12 illustrates that a system undergoing a Neimark-Sacker bifurcation can also display chaotic behavior

## 4. Results

The model of infectious disease spread, which includes vaccination and quarantine interventions alongside limited medical resources, demonstrates a dynamic system that can lead to chaotic outbreaks. Vaccination strategies can mitigate the impact of medical resource constraints by improving vaccine efficacy and administration rates. Additionally, controlling chaotic phenomena involves regulating infection rates within the population. Essentially, direct intervention in transmission rates is a key method for managing chaotic outbreaks. The general solution approach of linear parameter equation constraints shows that the explicit constrained mixed linear model is equivalent to the implicit constrained mixed linear model.

## References

[1] Q. Chen, Z. Teng, and F. Wang, "Fold-flip and strong resonance bifurcations of a discrete-time mosquito model," *Chaos Solitons Fractals*, vol. 144, p. 110704, Mar. 2021, [CrossRef].

[2] S. Işık, "A study of stability and bifurcation analysis in discrete-time predator–prey system involving the Allee effect," *International Journal of Biomathematics*, vol. 12, no. 01, p. 1950011, Jan. 2019, [CrossRef].

[3] P. A. Naik, Z. Eskandari, H. E. Shahkari, and K. M. Owolabi, "Bifurcation analysis of a discrete-time prey-predator model," *Bulletin of Biomathematics*, Oct. 2023, [CrossRef] .

[4] K. S. Al-Basyouni and A. Q. Khan, "Discrete-time COVID-19 epidemic model with chaos, stability and bifurcation," *Results Phys*, vol. 43, p. 106038, Dec. 2022, [CrossRef].

[5] G. Bucyibaruta, C. B. Dean, and M. Torabi, "A discrete-time susceptible-infectious-recovered-susceptible model for the analysis of influenza data," *Infect Dis Model*, vol. 8, no. 2, pp. 471–483, Jun. 2023, [CrossRef].

[6] S.-S. Zhou *et al.*, "Discrete-time macroeconomic system: Bifurcation analysis and synchronization using fuzzy-based activation feedback control," *Chaos Solitons Fractals*, vol. 142, p. 110378, Jan. 2021, [CrossRef].

[7] A. Q. Khan, S. M. Qureshi, and A. M. Alotaibi, "Bifurcation analysis of a three species discrete-time predator-prey model," *Alexandria Engineering Journal*, vol. 61, no. 10, pp. 7853–7875, Oct. 2022, [CrossRef].

[8] M. Zhao, "Bifurcation and chaotic behavior in the discrete BVP oscillator," *Int J Non Linear Mech*, vol. 131, p. 103687, May 2021, [CrossRef].

[9] L. H. A. Monteiro, "A discrete-time dynamical system with four types of codimension-one bifurcations," *Appl Math Comput*, vol. 354, pp. 189–191, Aug. 2019, [CrossRef].

[10] M. M. Aziz and O. M. Jihad, "Stability, Chaos Diagnose and Adaptive Control of Two Dimensional Discrete - Time Dynamical System," *OAlib*, vol. 08, no. 03, pp. 1–13, 2021, [CrossRef].

[11] Y. Lin, Q. Din, M. Rafaqat, A. A. Elsadany, and Y. Zeng, "Dynamics and Chaos Control for a Discrete-Time Lotka-Volterra Model," *IEEE Access*, vol. 8, pp. 126760–126775, 2020, [CrossRef].

[12] N. Parolini, L. Dede', G. Ardenghi, and A. Quarteroni, "Modelling the COVID-19 epidemic and the vaccination campaign in Italy by the SUIHTER model," *Infect Dis Model*, vol. 7, no. 2, pp. 45–63, Jun. 2022, [CrossRef].

[13] B. Yang, Z. Yu, and Y. Cai, "The impact of vaccination on the spread of COVID-19: Studying by a mathematical model," *Physica A: Statistical Mechanics and its Applications*, vol. 590, p. 126717, Mar. 2022, [CrossRef].

[14] F. Kemp *et al.*, "Modelling COVID-19 dynamics and potential for herd immunity by vaccination in Austria, Luxembourg and Sweden," *J Theor Biol*, vol. 530, p. 110874, Dec. 2021, [CrossRef].

[15] H. Moh and F. R. Fahreza, "Herd immunity in a coronavirus disease 2019 epidemic model with consideration of vaccination and quarantine interventions," *Advances in Differential Equations and Control Processes*, vol. 32, no. 1, p. 2759, Mar. 2025, [CrossRef].

[16] J. P. Gutiérrez-Jara, K. Vogt-Geisse, M. Cabrera, F. Córdova-Lepe, and M. T. Muñoz-Quezada, "Effects of human mobility and behavior on disease transmission in a COVID-19 mathematical model," *Sci Rep*, vol. 12, no. 1, p. 10840, Jun. 2022, [CrossRef].

[17] M. Ciotti, M. Ciccozzi, A. Terrinoni, W.-C. Jiang, C.-B. Wang, and S. Bernardini,

"The COVID-19 pandemic," *Crit Rev Clin Lab Sci*, vol. 57, no. 6, pp. 365–388, Aug. 2020, [CrossRef].

[18] R. B. Bestetti, R. Furlan-Daniel, and L. B. Couto, "Nonpharmaceutical public health interventions to curb the COVID-19 pandemic: a narrative review," *The Journal of Infection in Developing Countries*, vol. 16, no. 04, pp. 583–591, Apr. 2022, [CrossRef].

[19] D. Pradhan, P. Biswasroy, P. Kumar Naik, G. Ghosh, and G. Rath, "A Review of Current Interventions for COVID-19 Prevention," *Arch Med Res*, vol. 51, no. 5, pp. 363–374, Jul. 2020, [CrossRef].

[20] F. R. Fahreza, Moh. Hasan, and K. Kusbudiono, "Model and Simulation of COVID-19 Transmission with Vaccination and Quarantine Interventions in Jember," *InPrime: Indonesian Journal of Pure and Applied Mathematics*, vol. 5, no. 1, pp. 1–21, Jun. 2023, [CrossRef].

[21] M. Y. Li, *An Introduction to Mathematical Modeling of Infectious Diseases*. Cham: Springer International Publishing, 2018. [CrossRef].